frontiers | Frontiers in Plant Science

TYPE Original Research
PUBLISHED 27 February 2024
DOI 10.3389/fpls.2024.1332875

OPEN ACCESS

EDITED BY
Stefano Santabarbara,
National Research Council (CNR), Italy

REVIEWED BY
Milan Szabo,
Eötvös Loránd Research Network (ELKH), Hungary
Oded Liran,
University of Haifa, Israel

*CORRESPONDENCE
Fu-Biao Wang:
wfb19872856@163.com
Hua-Jing Kang
kanghuajing@126.com

†These authors have contributed equally to this work

RECEIVED 03 November 2023
ACCEPTED 02 February 2024
PUBLISHED 27 February 2024

CITATION
Ye Z-P, An T, Govindjee G, Robakowski P, Stirbet A, Yang X-L, Hao X-Y, Kang H-J and Wang F-B (2024) Addressing the long-standing limitations of double exponential and non-rectangular hyperbolic models in quantifying light-response of electron transport rates in different photosynthetic organisms under various conditions. *Front. Plant Sci.* 15:1332875. doi: 10.3389/fpls.2024.1332875

Addressing the long-standing limitations of double exponential and non-rectangular hyperbolic models in quantifying light-response of electron transport rates in different photosynthetic organisms under various conditions

Zi-Piao Ye[1†], Ting An[2†], Govindjee Govindjee[3], Piotr Robakowski[4], Alexandrina Stirbet[5], Xiao-Long Yang[6], Xing-Yu Hao[7], Hua-Jing Kang[8*] and Fu-Biao Wang[1*]

[1]The Institute of Biophysics in College of Mathematics and Physics, Jinggangshan University, Ji'an, Jiangxi, China, [2]School of Biological Sciences and Engineering, Jiangxi Agriculture University, Nanchang, China, [3]Plant Biology, Biochemistry, and Biophysics, University of Illinois at Urbana-Champaign, Urbana, IL, United States, [4]Faculty of Forestry and Wood Technology, Poznan University of Life Sciences, Poznan, Poland, [5]Retired, Newport News, VA, United States, [6]School of Life Sciences, University of Nantong, Nantong, Jiangsu, China, [7]College of Agriculture/State Key Laboratory of Sustainable Dry land Agriculture Jointly Built by the Shanxi Province and the Ministry of Science and Technology, Shanxi Agricultural University, Taiyuan, Shanxi, China, [8]Southern Zhejiang Key Laboratory of Crop Breeding of Zhejiang Province, Wenzhou Academy of Agricultural Sciences, Wenzhou, Zhejiang, China

The models used to describe the light response of electron transport rate in photosynthesis play a crucial role in determining two key parameters i.e., the maximum electron transport rate (J_{max}) and the saturation light intensity (I_{sat}). However, not all models accurately fit *J*–*I* curves, and determine the values of J_{max} and I_{sat}. Here, three models, namely the double exponential (DE) model, the non-rectangular hyperbolic (NRH) model, and a mechanistic model developed by one of the coauthors (Z-P Ye) and his coworkers (referred to as the mechanistic model), were compared in terms of their ability to fit *J*–*I* curves and estimate J_{max} and I_{sat}. Here, we apply these three models to a series of previously collected Chl *a* fluorescence data from seven photosynthetic organisms, grown under different conditions. Our results show that the mechanistic model performed well in describing the *J*–*I* curves, regardless of whether photoinhibition/dynamic down-regulation of photosystem II (PSII) occurs. Moreover, both J_{max} and I_{sat} estimated by this model are in very good agreement with the measured data. On the contrary, although the DE model simulates quite well the *J*–*I* curve for the species studied, it significantly overestimates both the J_{max} of *Amaranthus hypochondriacus* and the I_{sat} of *Microcystis aeruginosa* grown under NH_4^+-N supply. More importantly, the light intensity required to achieve the potential maximum of *J* (J_s) estimated by this model exceeds the unexpected high value of 10^5 μmol photons m^{-2} s^{-1} for *Triticum aestivum* and *A. hypochondriacus*. The NRH model fails to characterize

the *J-I* curves with dynamic down-regulation/photoinhibition for *Abies alba*, *Oryza sativa* and *M. aeruginosa*. In addition, this model also significantly overestimates the values of J_{max} for *T. aestivum* at 21% O_2 and *A. hypochondriacus* grown under normal condition, and significantly underestimates the values of J_{max} for *M. aeruginosa* grown under NO_3^-N supply. Our study provides evidence that the 'mechanistic model' is much more suitable than both the DE and NRH models in fitting the *J–I* curves and in estimating the photosynthetic parameters. This is a powerful tool for studying light harvesting properties and the dynamic down-regulation of PSII/photoinhibition.

KEYWORDS

double exponential model, dynamic down-regulation, electron transport rate, mechanistic model, non-rectangular hyperbolic model, photoinhibition

Introduction

Solar energy is an important environmental factor that drives charge separation in both photosystem I (PSI) and photosystem II (PSII) to produce electron transport rate, the *J* (see Table 1 for the list of abbreviations), which directly affects the subsequent formation of NADPH and ATP, as well as their allocation for carboxylation versus oxygenation of ribulose bisphosphate (RuBP) (Shevela et al., 2023). Chlorophyll *a* (Chl *a*) fluorescence is a valuable and sensitive tool for studying and understanding the electron transport process in photosynthesis, providing insights into the efficiency and functionality of electron transport and responses of photosynthetic organisms to changing environmental conditions (Mar and Govindjee, 1972; Govindjee, 1990, 2004; Baker, 2008; Stirbet et al., 2020). Moreover, the relationship between Chl *a* fluorescence and electron transport is complex and can be influenced by changes in environmental conditions, such as light intensity, temperature, and the availability of CO_2. Thus, accurately and rapidly characterizing the light-response curve of Chl *a* fluorescence (i.e., the *J–I* curve) of photosynthetic organisms can facilitate the assessment of their potential photosynthetic capacity over a wide range of ambient light intensities (White and Critchley, 1999; Maxwell and Johnson, 2000; Long and Bernacchi, 2003; Yin et al., 2009; von Caemmerer, 2013; Yin et al., 2021; Chang et al., 2023), which is crucial for optimizing agricultural productivity, studying ecosystem dynamics, and assessing the impact of environmental changes on photosynthetic processes.

Generally, for algae and cyanobacteria, the *J–I* curve is divided into three distinct parts depending on the light intensity levels: (1) light-limited, (2) light-saturated, and (3) photoinhibitory/dynamic down-regulation of PSII (Ralph and Gademann, 2005). The *J* level increases almost linearly with the increasing light intensity over the light-limited region until the light intensity reaches the saturation level (I_{sat}), after which the *J* level decreases with the increasing light intensity due to dynamic down-regulation of PSII/photoinhibition induced by high light intensity (Ralph and Gademann, 2005; Suggett et al., 2007; Yang et al., 2023). However, the division of the *J–I* curve for plants is much more complex (Robakowski, 2005; Ye et al., 2013a, b, 2016, 2019; Hu et al., 2021; He et al., 2022; Robakowski et al., 2022). Some plants show that the decrease in *J* with increasing light intensity is insignificant (Robakowski, 2005; Ye et al., 2013b; Robakowski et al., 2018; Ye et al., 2020); for some other plants, *J* fails to reach saturation even at the highest value of light intensity (Ye et al., 2013b; Buckley and Diaz-Espejo, 2015). Consequently, a robust *J–I* model should accurately provide the *J* responses to irradiance across all *I* levels and all patterns of *J–I* curves mentioned above. In addition, an ideal *J–I* model should also accurately determine two key parameters (i.e., I_{sat} and J_{max}) defining the *J–I* curves regardless of dynamic down-regulation of PSII/photoinhibition in the photosynthetic organisms under various environmental conditions.

Over the past 40 years, various models have been developed to characterize the *J–I* curves and estimate J_{max} and I_{sat}. Currently, the models for *J–I* curves of algae, cyanobacteria and plants are the double exponential model (referred to as DE model; Platt et al., 1980), the non-rectangular hyperbolic model (referred to as NRH model; von Caemmerer, 2000; Long and Bernacchi, 2003, 2013; Yin et al., 2009, 2021) which is a sub-model of FvCB model (Farquhar et al., 1980; von Caemmerer, 2000), a model developed by Ye et al. (Ye et al., 2013a, b) (referred to as a mechanistic model) and a few other models (e.g., single exponential model; Harrison and Platt, 1986; Robakowski, 2005). However, these models have been used differently; for example, the single exponential model has been shown to simulate *J–I* curves of algae, cyanobacteria, and plants, but it could obtain only the initial slope of the *J–I* curve (α) and the value of J_{max} (Rascher et al., 2000; Robakowski, 2005). The DE model has been mainly used for fitting the *J–I* curves of algae and cyanobacteria, and to provide values of J_{max}, I_{sat} and α (Ralph and Gademann, 2005). The NRH model has been extensively applied to

TABLE 1 Definitions of the abbreviations.

Abbreviation	Definition	Units
J	Electron transport rate	μmol electrons m^{-2} s^{-1}
J–I curve	Light response curve of electron transport	
J_{max}	Maximum electron transport rate	μmol electrons m^{-2} s^{-1}
J_s	Potential maximum electron transport rate	μmol electrons m^{-2} s^{-1}
α'	Allocation coefficient of light energy between PSII and PSI	dimensionless
β'	Leaf light absorption coefficient	dimensionless
N_0	Total number of photosynthetic pigment molecules	
φ	Use efficiency of exciton transport reaction center PSII to cause charge separation of P680	dimensionless
τ	Average life-time of the photosynthetic pigment molecules in the excited state k	s
σ_{ik}	Eigen-absorption cross-section of photosynthetic pigment molecule from ground state i to excited state k	m^2
g_i	Degeneration of energy level of photosynthetic pigment molecules in the ground state i	dimensionless
g_k	Degeneration of energy level of photosynthetic pigment molecules in the excited state k	dimensionless
k_P	Rate of pigment molecules for the transfer of the excited state k to the ground state i due to photochemical reaction	s^{-1}
k_D	Rate of pigment molecules for the transfer of the excited state k to the ground state i due to non-radiation heat dissipation	s^{-1}
ξ_1	Occupation probabilities of photochemistry	dimensionless
ξ_2	Occupation probabilities of non-radiation heat dissipation	dimensionless
ξ_3	Occupation probabilities of fluorescence	dimensionless
I	Light intensity	μmol photons m^{-2} s^{-1}
I_{sat}	Saturation light intensity corresponding to J_{max}	μmol photons m^{-2} s^{-1}
PSII	Photosystem II	
α	Initial slope of light-response curve of electron transport rate	μmol electrons (μmol photons)$^{-1}$
β	Photoinhibition term	μmol electrons (μmol photons)$^{-1}$
γ	Light-saturated coefficient	μmol electrons (μmol photons)$^{-1}$
θ	Convexity	dimensionless

fit the J–I curves of plants, but it has only provided values of α and J_{max} (Long and Bernacchi, 2003; von Caemmerer, 2013; Ye et al., 2019; Yin et al., 2021). However, the mechanistic model (developed by Ye et al., 2013a, b) has been found to be increasingly of use in simulating the J–I curves of algae, cyanobacteria, and plants, as well as in obtaining the values of α, J_{max} and I_{sat} (Serodio et al., 2013; Ye et al., 2013a; Morfopoulos et al., 2014; Sun et al., 2015; Ahammed et al., 2018; Robakowski et al., 2018; Yang et al., 2018; Ye et al., 2019; Robakowski et al., 2022; Yang et al., 2023). These models provide valuable tools for understanding the photosynthetic performance of different photosynthetic organisms under various environmental conditions.

The establishment of different J-I models is based on different photosynthetic tissues and photosynthetic units. For example, the DE model is mainly constructed based on the photosynthetic characteristics of algae and cyanobacteria, with the photosynthetic factory as the basic unit (Platt et al., 1980; Eilers and Peeters, 1988). The NRH model, on the other hand, is based on the photosynthetic characteristics of C_3 plants (von Caemmerer, 2000; Long and Bernacchi, 2003; von Caemmerer, 2013). It is not yet known, however, whether the differences in models establishment is the reason why the DE model is only limited to simulate the J–I curve of algae and cyanobacteria, but not of the plants, and why the NRH model has only been used for fitting the J–I curves of C_3 plants but not of algae and cyanobacteria. Although the mechanistic model is based more on the photosynthetic characteristics of C_3 and C_4 plants, with individual photosynthetic pigment molecules as the basic unit (Ye et al., 2013a, b), it is unclear whether the mechanistic model can accurately and precisely fit all types of J–I curves mentioned above, and whether the values of J_{max} and I_{sat} fitted with this model are close to the corresponding observed values, and whether there is any significant difference between the fitted values of J_{max} and I_{sat} and their corresponding observed values.

To our knowledge, the aforementioned models have not yet been applied to compare the measured (observed) values of the cardinal points of light response curves with the values simulated with the models using the taxa of photosynthetic organisms from the different functional groups: evergreen conifer trees, crops, C_3 and C_4 plants, ornamental plants and algae. Thus, the goal of this study was to evaluate the performance of the mechanistic model versus the most widely used DE and NRH models for the I level from zero to a high level of irradiance, using the experimental data

collected on seven different photosynthetic species under various environmental conditions. In addition, to consider a broader range of model comparisons, we also compared the Eilers and Peeters model (referred to as EP model; Eilers and Peeters, 1988) with the mechanistic model. Despite the fact that the EP model represents the relationship between light intensity and the rate of photosynthesis in algae and phytoplankton (Eilers and Peeters, 1988; Schreiber and Klughammer, 2013), we found that the model can also fit the *J-I* curve if we consider the rate of photosynthesis as *J*. We have presented the fitting results of the EP model in the Supporting Information.

Materials and methods

Chl *a* fluorescence parameters were collected from seven different photosynthetic organisms. The detailed growth conditions, measurement methods, parameter settings, and fitting methods of the *J-I* curve for each of the photosynthetic species are described below:

(i) *Abies alba* Mill., which follows the C_3 carboxylation pathway, was grown under high light (HL) condition representing 100% of full sun irradiation, and low light (LL) condition representing 40% of full sun irradiation in Poznan, western Poland. The Chl *a* fluorescence was determined using a fluorescence monitoring system (FMS 2, Hansatech, Norfolk, UK). The fully expanded current-year needles were subjected to a dark adaptation at room temperature (21-23 °C) for 30 minutes. The measurements of Chl *a* fluorescence were conducted using modulated and saturated light intensities set at 0.05 μmol photons m^{-2} s^{-1} and 15.3 mmol photons m^{-2} s^{-1}, respectively. Other parameters of the instrument were set following the method of Robakowski et al. (2022). The electron transport rates (*ETR*) were calculated using the formula $ETR = \alpha \times \Phi_{PSII} \times PPF \times 0.5$, as proposed by Maxwell and Johnson (2000). Here, α refers to needle absorptance, Φ_{PSII} denotes the quantum yield of PSII, *PPF* represents the photosynthetic photon flux of actinic light. Assumptions were made that the excitation energy is partitioned equally between the two photosystems (hence the factor of 0.5; Maxwell and Johnson, 2000).

(ii) Two rice (*Oryza sativa* L.) varieties, which follow the C_3 carboxylation pathway, are Wufengyou 1326 and Ganfengyou 1326 (Ye et al., 2019). In 2014, the rice seedlings were planted at Jinggangshan University experimental farm in Ji'an city, Jiangxi Province, China. The farm had moderate soil fertility, and field management followed the local rice planting process, including regular water and timely weed control. Healthy rice flag leaves, with similar growth, were selected and tagged during the heading stage. The *J* level of the rice leaves at the dough stage was measured using a portable photosynthesis analyzer (LI-6400, Li-Cor INC. USA) with a fluorescence leaf chamber (LI-6400-40). The CO_2 flow rate in the leaf chamber was set at 390 μmol mol^{-1}, the temperature of the leaf chamber was set at 30 °C, and the photosynthetically active radiation (*PAR*) was set at 2000, 1800, 1600, 1400, 1200, 1000, 800, 600, 400, 200, 150, 100, 50 and 0 μmol photons m^{-2} s^{-1}.

(iii) *Triticum aestivum* L., which follows the C_3 carboxylation pathway, was 'Qimai 22'. Seeds were sown in October 2011 with regular field management practices. When the wheat was in the flowering stage, healthy and similarly grown plants, randomly selected, were chosen for the measurement of Chl *a* fluorescence. The *J-I* curves of flag leaves were determined using a portable photosynthesis/fluorescence analyzer (LI-6400, Li-Cor INC. USA). The temperature in the leaf chamber was set at 33 °C, The CO_2 flow rate was set at 380 μmol mol^{-1}, and the *PAR* was set at 2000, 1800, 1600, 1400, 1200, 1000, 800, 600, 400, 200, 150, 100, 50 and 0 μmol photons m^{-2} s^{-1} (Kang et al., 2019).

(iv) The variety of *Setaria italica* L., which follows the C_4 carboxylation pathway, used was 'An 04'. The experiment was conducted at the experimental base of Shanxi Agricultural University in Taiyuan city, Shanxi Province, China. Seeds were sown in plastic barrels with a diameter and height of 0.28×0.26 m. After the seedlings had three true leaves, the experimental treatments were performed. Two moisture treatments were set: non-drought stress (normal watering) and drought stress. The relative leaf water content was used to measure the degree of drought stress on the plants. The fully expanded reverse second leaves were selected for measuring the *J-I* curves using a portable photosynthesis/fluorescence analyzer (LI-6400XT, Li-Cor INC. USA) during the heading stage. The CO_2 flow rate was set at 500 μmol mol^{-1}, and the *PAR* was set at 2000, 1800, 1600, 1200, 800, 600, 400, 200, 100 and 0 μmol photons m^{-2} s^{-1} during the measurement (Feng et al., 2022).

(v) In another experiment, *Zea mays* L., specifically the 'KFJT-1' variety with a C_4 carboxylation pathway, was used. The seeds were sown in a growth chamber with a light intensity set at 1500 LUX after seeds germination. The daily light cycle consisted of 13 hours of light and 11 hours of darkness. After one month of plant growth, one healthy leaf was selected from each plant for Chl *a* fluorescence measurement using a portable photosynthesis/fluorescence measurement system (Li-6800-01A, Li-Cor INC. USA). The CO_2 flow rate in the leaf chamber was set at 500 μmol mol^{-1}, and the relative humidity was controlled at around 70%. The measurement was conducted using the built-in program of the instrument, with the light intensity gradient set at 2000, 1800, 1600, 1400, 1200, 1000, 800, 600, 400, 200, 150, 100, 50, 25 and 0 μmol photons m^{-2} s^{-1} (Wang et al., 2022).

(vi) The grain amaranth (*Amaranthus hypochondriacus* L.), which follows the C_4 carboxylation pathway, was planted in the field at the Yucheng Comprehensive Experiment Station of the Chinese Academy of Sciences. The light intensity in this region usually reaches around 2000 μmol

photons m^{-2} s^{-1} during the growing season. The seedlings were planted on June 15th 2012, and promptly watered during the entire experimental period. The Chl *a* fluorescence of the fully expanded sun-exposed leaves was measured using a portable photosynthesis/fluorescence analyzer (LI-6400, Li-Cor INC. USA) after 45 days of planting in the field. The *J-I* curves of the leaves were measured using the built-in program of the instrument, with the CO_2 flow rate maintained at 380 μmol mol^{-1}, the temperature of the leaf chamber at 35 °C, and the light intensity gradient set at 2000, 1800, 1600, 1400, 1200, 1000, 800, 600, 400, 200, 150, 100, 50, 25 and 0 μmol photons m^{-2} s^{-1} (Ye et al., 2020).

(vii) *Microcystis aeruginosa* FACHB905 used in our experiment, which follows C_3 carboxylation pathway, was obtained from the Freshwater Algae Culture Collection of the Institute of Hydrobiology, Chinese Academy of Sciences. After two generations of propagation on BG11 medium, algal cells, in the mid-exponential growth phase, were collected for the experiment. The algal cells were subjected to starvation treatment and then inoculated into the BG11 medium, containing 10 ml g^{-1} of NO_3^-N ($NaNO_3$) or 10 ml/g of NH_4^+-N (NH_4Cl). When the algal density reached 1.8×10^6 cells mL^{-1}, the *J-I* curves of the algal were measured with the built-in program of a Phyto-PAM fluorescence monitoring system manufactured by Walz Germany (Yang et al., 2023).

Data processing and statistical analysis

The *J–I* curves (of Chl *a* fluorescence transient) of all the collected data have been fitted by the DE, NRH and mechanistic models to obtain the key parameters defining the *J–I* curves, using the *Photosynthesis Model Simulation Software* (PMSS), which is available in both Chinese and English versions (http://photosynthetic.sinaapp.com, Jinggangshan University, Ji'an).

All the statistical tests were performed using the *SPSS 18.5* statistical software package (*SPSS*, Chicago, IL). Student's *t*-test was used to test whether there were significant differences between the fitted and measured values of the quantitative traits, such as J_{max} and I_{sat}. Goodness of fit of the mathematical model to the experimental observations was assessed using the coefficient of determination (R^2 = 1 – SSE/SST, where SST is the total sum of squares and SSE is the error sum of squares) with probability obtained in the analysis of variance.

Examples of model application

The mechanistic model of *J–I* curve of Chl *a* fluorescence can be described as (Ye et al., 2013a, b):

$$J = \frac{\alpha'\beta' N_0 \sigma_{ik} \varphi}{S} \times \frac{1 - \frac{(1-g_i/g_k)\sigma_{ik}}{\xi_3 + (\xi_1 k_P + \xi_2 k_D)\tau} I}{1 + \frac{(1+g_i/g_k)\sigma_{ik}}{\xi_3 + (\xi_1 k_P + \xi_2 k_D)\tau} I} I \quad (1)$$

The definitions and units of the parameters in the Equation 1 are listed in the Table 1. According to Ye et al (Ye et al., 2013a, b), α' was defined as the allocation coefficient of light energy between PSII and PSI (dimensionless); β' was defined as the leaf light absorption coefficient (dimensionless); $N_0$was defined as the total number of photosynthetic pigment molecules; σ_{ik} was defined as the eigen-absorption cross-section of photosynthetic pigment molecule from ground state *i* to excited state *k* (unit: m^2), representing the ability of plant pigment molecules to absorb light energy, and the values may vary among different plants and algae; φ was defined as the use efficiency of excitons transport reaction center PSII to cause charge separation at P680 (dimensionless); g_i and g_k were defined as the degeneration of energy level of photosynthetic pigment molecules in the ground state *i* and excited state *k* (dimensionless), respectively; ξ_1, ξ_2, and ξ_3 were the occupation probabilities of photochemistry, non-radiation heat dissipation, and fluorescence (dimensionless), respectively; k_P was defined as the rate of pigment molecules from the excited state *k* to the ground state *i* due to photochemical reaction (unit: s^{-1}); k_D was defined as the rate of pigment molecules from the excited state *k* to the ground state *i* due to non-radiation heat dissipation (unit: s^{-1}); τ was defined as the average life-time of the photosynthetic pigment molecules in the excited state *k* (unit: s). α', β', N_0, σ_{ik}, φ, g_i, g_k, ξ_1, ξ_2, ξ_3, k_P, k_D and τ in the mechanistic model are used to characterize the intrinsic properties of chlorophyll molecules, and their values vary and depend on photosynthetic species and environmental conditions. But for a given species under specific conditions, we can assume that $\alpha = \frac{\alpha'\beta' N_0 \sigma_{ik} \varphi}{S}$(μmol electron (μmol photons)$^{-1}$) was defined as the initial slope of the *J–I* curve, $\beta = \frac{(1-g_i/g_k)\sigma_{ik}\tau}{\xi_3 + (\xi_1 k_P + \xi_2 k_D)\tau}$((μmol photons)$^{-1}$ m^2 s) was defined as the "dynamic down-regulation term of PSII/photoinhibition", and $\gamma = \frac{(1+g_i/g_k)\sigma_{ik}\tau}{\xi_3 + (\xi_1 k_P + \xi_2 k_D)\tau}$ ((μmol photons)$^{-1}$ m^2 s) was defined as "the saturation term of photosynthesis" (Ye et al., 2013a, b). Then, the Equation 1 can be simplified as:

$$J = \alpha \frac{1 - \beta I}{1 + \gamma I} I \quad (2)$$

Taking the first derivative of Equation 2 yields the following formula:

$$J' = \alpha \frac{1 - 2\beta I - \beta\gamma I^2}{(1 + \gamma I)^2} \quad (3)$$

Since the first derivative of Equation 3 can be equal to zero and its second derivative can be less than zero, we suggest that Equation 3 has critical points, which can be used to calculate the values of I_{sat} and J_{max} of photosynthetic organisms. Therefore, when setting Equation 3 equal to zero, the I_{sat} can be calculated as:

$$I_{sat} = \frac{\sqrt{(\beta + \gamma)/\beta} - 1}{\gamma} \quad (4)$$

Substituting Equation 4 into Equation 2, the J_{max} can be calculated as:

$$J_{max} = \alpha \left(\frac{\sqrt{\beta + \gamma} - \sqrt{\beta}}{\gamma} \right)^2 \quad (5)$$

According to Ye et al (Ye et al., 2013a, b), the coefficients in the mechanistic model have specific biological significance. (1) When $I < I_{sat}$, J increases with increasing I. The slopes of this increasing part of curves can be compared among species or among ecotypes within the same species, under different environmental conditions or experimental treatments. This suggests that the response of J to increasing I can vary among species or among ecotypes within a species. (2) When $I = I_{sat}$, J reaches its maximum value J_{max} (Equation 5), the values of J_{max} are species-specific and also vary within the species reflecting adaptation to the light environment. Different species may have different J_{max}, indicating their specific abilities to utilize light for photosynthesis. (3) When $I > I_{sat}$, the photosynthetic organisms undergo photoinhibitory/dynamic down-regulation of PSII, and J decreases with increasing I. The value of photoinhibition term (β, Equation 2) depends on species, intraspecific variation and environmental factors, especially on the light level. This is species-specific and provides the information about the species' tolerance to the photoinhibitory conditions (high light, low temperature, drought). In summary, the species-specific differences in the response of J to increasing light intensity (I) and the values of J_{max} and photoinhibition (β) in the mechanistic model indicate the specific biological adaptations and tolerances of different species to their light environments.

In Figure 1, we show the J–I curve (fitting with the mechanistic model) for three C_3 species (i.e., *Abies alba* Mill., *Oryza sativa* L. and *Triticum Aestivum* L.), three C_4 species (i.e., *Setaria italica* L., *Zea mays* L. and *Amaranthus hypochondriacus* L.) and for one cyanobacterium (*Microcystis aeruginosa* FACHB905). The three distinct parts of J–I curves such as the light-limited, light-saturated and photoinhibitory regions are shown for *A. alba* grown under LL (Figure 1A), for *O. sativa* grown under normal conditions (Figure 1B) and *M. aeruginosa* grown under two different nitrogen supplies (Figure 1F). On the other hand, *A. alba* grown under HL (Figure 1A), *T. aestivum* at 2% O_2 (Figure 1C), *S. italica* under non-drought (normal water) conditions (Figure 1D) and *Z. mays* grown under normal conditions (Figure 1E) exhibited a small decline of the J level with increasing light intensity beyond the I_{sat}. Data for *T. aestivum* at 21% O_2 (Figure 1C), for *S. italica* under drought stress (Figure 1D) and *Z. mays* grown under normal conditions (Figure 1E) show that the J level hardly increases with increasing light intensity beyond the I_{sat}. However, we note that the J level for *T. aestivum* at 21% O_2 (Figure 1C) as well as for *A. hypochondriacus* grown under normal conditions (Figure 1E) reaches saturation at about 2000 µmol photons m^{-2} s^{-1}. Moreover, the fitted curves demonstrate that the mechanistic model fits quite well the J–I curves of all the seven species, regardless of whether photoinhibition/dynamic down-regulation occurs, or not, and this with extremely good fits ($R^2 \geq 0.994$) (Figure 1; Table 2). Furthermore, the results fitted by the mechanistic model in Table 2 show that the photosynthetic parameters (e.g., J_{max} and I_{sat}) of the seven species are in very close agreement with their corresponding observed values, and that

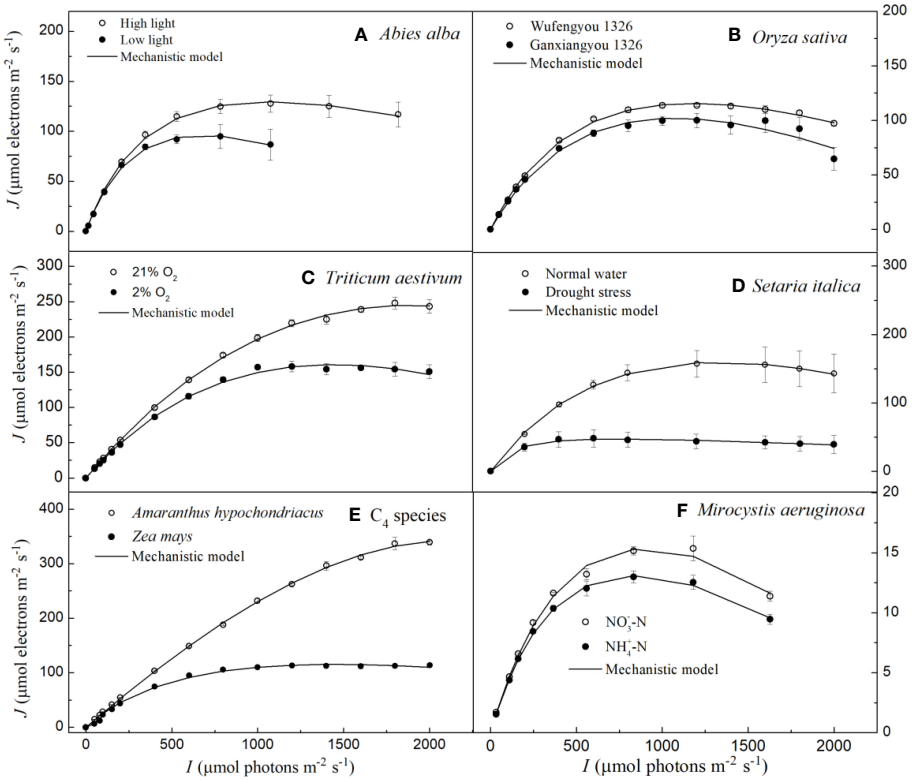

FIGURE 1
Light response curves of photosynthetic electron fitted by the mechanistic model for seven species under various environmental conditions (means ± SE, n = 3 - 6). **A**, *Abies alba*; **B**, *Oryza sativa*; **C**, *Triticum aestivum*; **D**, *Setaria italica*; **E**, C4 species; **F**, *Microcystis aeruginosa*.

TABLE 2 Results fitted by the mechanistic model and observation values of photosynthetic parameters for seven species under various conditions (mean ± *SE*, *n* = 3-6).

	A. alba				*O. sativa*				*T. aestivum*			
	LL		HL		Wufengyou 1326		Ganfengyou 1326		2% O_2		21% O_2	
	Mechanistic model	Obs.	Mechanistic model	Obs.	Mechanistic model	Obs.	Mechanistic model	Obs.	Mechanistic model	Obs.	Mechanistic model	Obs.
α	0.520 ±0.013	–	0.488 ±0.008	–	0.321 ±0.003	–	0.281 ±0.005	–	0.282 ± 0.012	–	0.295 ± 0.012	–
I_{sat}	831.29 ±205.65[a]	796.00 ±157.46[a]	1076.68 ±40.48[a]	1094.20 ±141.40[a]	1181.05 ±11.32[a]	1133.82 ±133.12[a]	1076.22 ±13.35[a]	1200.59 ±199.73[a]	1453.54 ± 53.59a	1400.00 ± 141.42a	1927.19 ± 77.69a	1840.00 ± 74.83a
J_{max}	96.91 ±5.01a	94.99 ±5.31a	129.71 ±3.94a	127.87 ±3.76a	115.63 ±2.16[a]	113.64 ±2.17[a]	102.48 ±0.58[a]	105.50 ±7.39[a]	161.58 ± 5.62a	158.08 ± 7.69a	246.27 ± 7.63a	248.12 ± 8.39a
R^2	0.999	–	0.999	–	0.999	–	0.996	–	0.997	–	0.999	–
	S. italica				*Z. mays*		*A. hypochondriacus*		*M. aeruginosa*			
	Normal water		Drought stress						NO^-_3-N		NH_4^+-N	
	Mechanistic model	Obs.	Mechanistic model	Obs.	Mechanistic model	Obs.	Mechanistic model	Obs.	Mechanistic model	Obs.	Mechanistic model	Obs.
α	0.345 ± 0.005	–	0.477 ± 0.031	–	0.286 ±0.013	–	0.282 ±0.012	–	0.050 ±0.001	–	0.049 ±0.001	–
I_{sat}	1329.47 ± 107.53[a]	1399.75 ± 198.60[a]	737.78 ± 57.21[a]	601.07 ± 0.31[a]	1446.78 ±16.87[a]	1399.99 ±200.01[a]	2100.22 ±23.90[a]	1933.33 ±67.02[a]	904.45 ±3.89[a]	949.00 ±116.00[a]	840.21 ±7.73[a]	833.00 ±0.00[a]
J_{max}	160.30 ± 14.98[a]	158.72 ± 15.29[a]	47.28 ± 8.06[a]	48.19 ± 8.89[a]	115.33 ±1.02[a]	113.95 ±1.03[a]	341.99 ±6.39[a]	342.91 ±8.02[a]	15.37 ±0.49[a]	15.65 ±0.61[a]	13.09 ±0.81[a]	12.99 ±0.49[a]
R^2	0.997	–	0.999	–	0.999	–	0.999	–	0.994	–	0.996	–

α, initial slope of -I curves; I_{sat}, saturation irradiance (μmol photons m^{-2} s^{-1}); J_{max}, maximum electron transport rate (μmol electrons m^{-2} s^{-1}); R^2, determination coefficient. The different superscript letters followed by the values are significantly different between fitted values and observation values for the same species or the same species under the same treatment ($p < 0.05$).

10.3389/fpls.2024.1332875

there is no significant difference between the fitted values of J_{max} (and I_{sat}) of the seven species and their corresponding observed values (Table 2; Supplementary Table S2).

We further conducted a comparison between the fits of the *J–I* curves obtained from our mechanistic model and those obtained from a highly classic DE model. We note that the DE model has been earlier used to simulate the *J–I* curves in algae and cyanobacteria (Platt et al., 1980; Harrison and Platt, 1986; Henley, 1993; Rascher et al., 2000; Ralph and Gademann, 2005; Karageorgou and Manetas, 2006; Yang et al., 2023), but rarely in plants due to differences in the physiology and light response characteristics of these photosynthetic species. The DE model is expressed as follows:

$$J = J_s(1 - \exp(-\alpha I/J_s))\exp(-\beta I/J_s) \quad (6)$$

where, J_s is a parameter reflecting the maximum, potential, light saturated *J*, α (>0) is the initial slope (μmol electrons (μmol photons)$^{-1}$) of the *J-I* curve, β (>0; in μmol electrons (μmol photons)$^{-1}$) is used to represent the photoinhibition term (Harrison and Platt, 1986) or dynamic down-regulation of PSII (Ralph and Gademann, 2005), obtained from the slope of the *J–I*, when the PSII activity decreases (Henley, 1993). If $\beta = 0$, Equation 6 becomes a single exponential model (Harrison and Platt, 1986). In this case, theoretically, J_s must be equal to J_{max}, but, it also means that the light intensity (I_{sat}) at which the electron transport rate saturates (J_{max}) cannot be calculated since there is no inflection point in the *J-I* curve fitted by the single exponential to determine a saturation point.

Based on Equation 6, the parameters I_{sat} and J_{max} were calculated by Equation 7 and Equation 8, respectively:

$$I_{sat} = \frac{J_s}{\alpha}\ln\frac{\alpha+\beta}{\beta} \quad (7)$$

And

$$J_{max} = J_s\frac{\alpha}{\alpha+\beta}\left(\frac{\beta}{\alpha+\beta}\right)^{\beta/\alpha} \quad (8)$$

We note that the DE model has been widely used to fit the *J–I* curves of algae and cyanobacterium (Platt et al., 1980; Harrison and Platt, 1986; Henley, 1993; Ralph and Gademann, 2005). Our results show that although it simulates *J–I* curves of plants well with high R^2, it significantly overestimates both J_{max} and I_{sat} for *A. hypochondriacus* growing under normal conditions (Figure 2, Table 3). Further, there is a significant difference between the estimated J_{max} and I_{sat} and their corresponding observed values (Tables 3, S2). On the other hand, for *M. aeruginosa* grown under NH^+_4-N supply, the model significantly underestimates I_{sat} (Table 3; Supplementary Table S2). Although I_{sat} and J_{max} can be calculated by Equation 7 and Equation 8, respectively, and there are no significant differences between the estimated and the observed values of I_{sat} and J_{max} for all the species except for *A. hypochondriacus* growing under normal conditions, and for *M.*

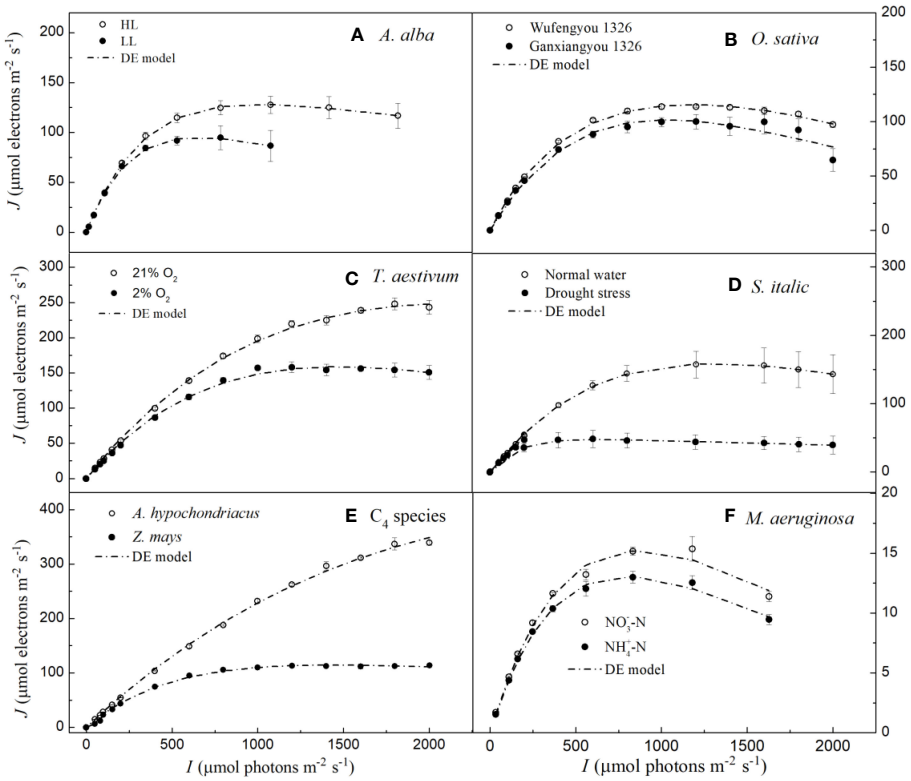

FIGURE 2
Light response curves of photosynthetic electron fitted by the DE model for seven species under various environmental conditions (means ± SE, *n* = 3 - 6). **A**, *Abies alba*; **B**, *Oryza sativa*; **C**, *Triticum aestivum*; **D**, *Setaria italica*; **E**, C4 species; **F**, *Microcystis aeruginosa*.

TABLE 3 Results fitted by DE model and observation values of photosynthetic parameters for seven species under various conditions (mean ± *SE*, *n* = 3-6).

	A. alba				*O. sativa*				*T. aestivum*			
	LL		HL		Wufengyou 1326		Ganfengyou 1326		$2\%O_2$		$21\%O_2$	
	DE model	Obs.	DE model	Obs.	DE model	Obs.	DE model	Obs.	DE model	Obs.	DE model	Obs.
α	0.452 ± 0.007	–	0.452 ± 0.007	–	0.305 ± 0.005	–	0.269 ± 0.004	–	0.293 ± 0.011	–	0.309 ± 0.013	–
β	0.320 ±0.005	–	0.032 ±0.005	–	0.081 ±0.003	–	68.35 ±12.51	–	(3.26±1.55)′10^3	–	(5.06 ±1.58)′10^3	–
I_{sat}	804.62 ±43.92[a]	796.00 ±157.46[a]	1015.09 ±46.31[a]	1094.20 ±141.40[a]	1130.58 ±140.58[a]	1133.82 ±133.12[a]	1039.44 ±25.78[a]	1200.59 ±199.73[a]	1474.81 ± 73.91[a]	1400.00 ± 141.42[a]	2193.89 ± 79.87[a]	1840.00 ± 74.83[a]
J_{max}	93.98 ±8.21[a]	94.99 ±5.31[a]	128.48 ±3.58[a]	127.87 ±3.76[a]	115.54 ±1.45a	113.64 ±2.17[a]	102.59 ±7.21[a]	105.50 ±7.39[a]	158.80 ± 4.65[a]	158.08 ± 7.69[a]	249.25 ± 7.89[a]	248.12 ± 8.39[a]
J_s	297.05 ±6.77	-	166.24 ±3.52	–	221.26 ±5.81	–	75.56 ±5.89	–	(4.81±1.56)′10^6	–	(1.10 ±0.34)′10^7	–
R^2	0.998	-	0.999	–	0.981	–	0.996	–	0.997	–	0.999	–
	S. italica				*Z. mays*		*A. hypochondriacus*		*M. aeruginosa*			
	Normal water		Drought stress						NO^-_3-N		NH_4^+-N	
	DE model	Obs.	DE model	Obs.	DE model	Obs.	DE model	Obs.	DE model	Obs.	DE model	Obs.
α	0.333 ± 0.001	–	0.323 ± 0.031	–	0.227 ±0.010	–	0.300 ±0.002	–	0.048 ±0.000	–	0.046 ±0.001	–
β	(1.93 ±0.25)×10^2	–	(8.21 ±0.69)×10^{-3}	–	0.023 ±0.008	–	(2.39 ±1.36)×10^4	–	(2.25 ±3.28)×10^5	–	0.082 ±0.088	–
I_{sat}	1305.31 ± 119.69[a]	1399.75 ± 198.60[a]	608.21 ± 48.77[a]	601.07 ± 0.31[a]	1444.33 ±29.86[a]	1399.99 ±200.01[a]	3701.88 ±67.37[a]	1933.33 ±67.02[b]	864.05 ±2.73[a]	949.00 ±116.00[a]	795.64 ±9.63[b]	833.00 ±0.00[a]
J_{max}	159.69 ± 14.67[a]	158.72 ± 15.29[a]	47.53 ± 8.03a	48.19 ± 8.89[a]	114.51 ±0.92[a]	113.95 ±1.03[a]	408.11 ±10.29[a]	342.91±8.02[b]	15.18 ±0.39[a]	15.65 ±0.61[a]	13.09 ±0.58[a]	12.99 ±0.49[a]
J_s	(2.75 ±2.72) ×10^6	–	53.52 ±8.92	–	154.19 ±11.22	–	(9.68 ±3.27) ×10^5	–	(1.94 ±2.84)×10^8	–	81.74±73.23	–
R^2	0.997	–	0.999	–	0.999	–	0.999	–	0.943	–	0.995	–

J_s, potential maximum electron transport rate (μmol photons m^{-2} s^{-1}); β, the photoinhibition coefficient; for other abbreviations, see Table 2. The different superscript letters followed by the values are significantly different between fitted values and observation values for the same species or for the same species under the same treatment ($p < 0.05$).

10.3389/fpls.2024.1332875

aeruginosa grown under NH^+_4-N supply (for I_{sat}), J_s estimated by the DE model is significantly greater than the J_{max} (Table 3), especially for *T. aestivum* (grown at 2% O_2 and 21% O_2), *Z. mays* (grown under normal conditions), and even *M. aeruginosa* (grown under different nitrogen treatments) (Table 3). For instance, for *T. aestivum*, grown at 2% O_2 and 21% O_2, the values of J_s estimated by the DE model are 4.81×10^6 and 1.10×10^7 µmol photons m^{-2} s^{-1} (Table 3), respectively. However, for *T. aestivum*, grown at 2% O_2 and 21% O_2, the observed values of J_{max} are 158.08(± 7.69) and 248.12 (± 8.39) µmol photons m^{-2} s^{-1}, respectively. In addition, when we fit the *J–I* curves of *T. aestivum* (grown at 2% O_2 and 21% O_2) by a single exponential model ($J = J_{max}(1 - \exp(-\alpha I/J_{max}))$), the values of J_{max} are 164.55 and 280.25 µmol photons m^{-2} s^{-1}, respectively. For *O. sativa* cv Ganfengyou 1326 (grown under normal conditions), J_s estimated by the DE model is 75.56 (±5.89) µmol photons m^{-2} s^{-1}, which is, however, significantly lower than its observed value of J_{max} (105.50 (±7.39) µmol photons m^{-2} s^{-1}) (Table 3).

Compared with the DE model which has been widely used to fit *J–I* curves of algae and cyanobacteria, the NRH model (von Caemmerer, 2000) has been mainly used to fit the *J–I* curves of plants (von Caemmerer, 2000; Long and Bernacchi, 2003; Miao et al., 2009; Gu et al., 2010; Bernacchi et al., 2013; von Caemmerer, 2013; Buckley and Diaz-Espejo, 2015; Cai et al., 2018; Yin et al., 2021). The NRH model gives the values of '*J*' and d*J*/d*I* (Equation 9 and Equation 10, respectively; for further information, see von Caemmerer (von Caemmerer, 2000, 2013) and Yin et al. (2021)).

$$J = \frac{\alpha I + J_{max} - \sqrt{(\alpha I + J_{max})^2 - 4\alpha\theta J_{max} I}}{2\theta} \quad (9)$$

where, α is the initial slope of the *J–I* curve (µmol electrons (µmol photons)$^{-1}$), and θ ($0<\theta<1$) is the curve convexity.

The first derivative of Equation 9 is:

$$\frac{dJ}{dI} = \frac{\alpha}{2\theta}\left[1 - \frac{(\alpha I + J_{max}) - 2\theta J_{max}}{\sqrt{(\alpha I + J_{max})^2 - 4\theta\alpha I J_{max}}}\right] \quad (10)$$

where, dJ/dI equals to α if I is zero, and $dJ/dI > 0$ if $I>0$. We note that Equation 9 is an asymptote function that fails to determine the I_{sat}.

In Figure 3, we can observe that the NRH model fails to fit the *J-I* curves of the plant species and cyanobacteria under dynamic down-regulation of PSII/photoinhibition conditions, and it overestimates J_{max} for *T. aestivum* grown at 21% O_2 and *A. hypochondriacus* grown under normal conditions, and there is a significant difference between the estimated and observed J_{max} values for each species ($p< 0.05$) (Table 4; Supplementary Table S2). Moreover, this model significantly underestimates J_{max} for *M. aeruginosa* grown under NO^-_3-N supply, with a notable discrepancy between the estimated and observed J_{max} values ($p< 0.05$) (Table 4).

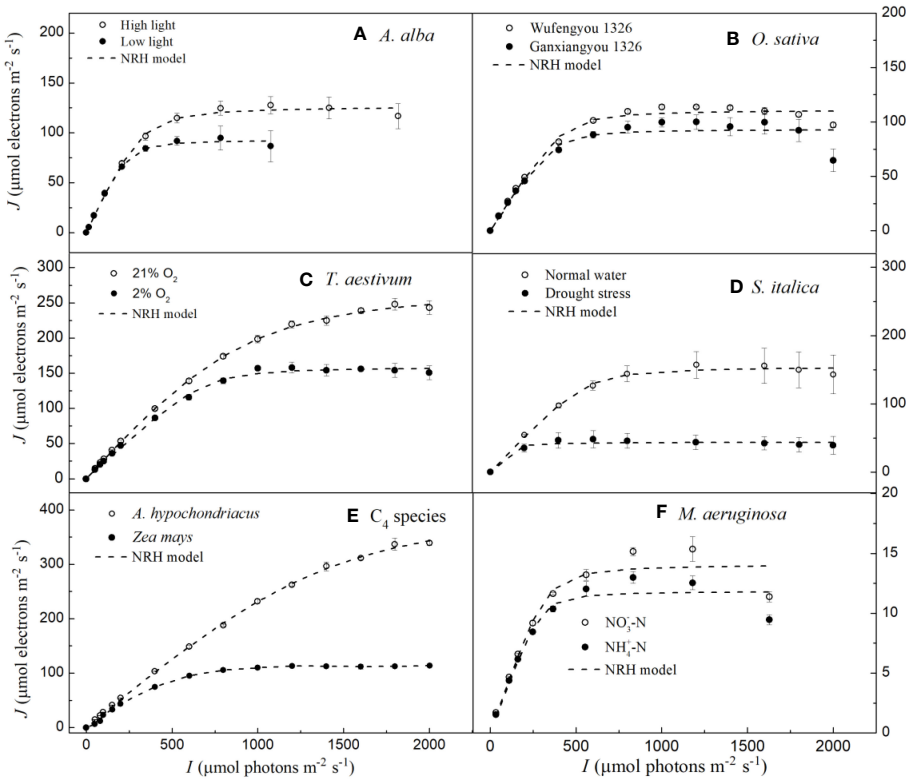

FIGURE 3
Light response curves of photosynthetic electron fitted by the NRH model for seven species under various environmental conditions (means ± SE, n = 3 - 6). **A**, *Abies alba*; **B**, *Oryza sativa*; **C**, *Triticum aestivum*; **D**, *Setaria italica*; **E**, C4 species; **F**, *Microcystis aeruginosa*.

TABLE 4 Results fitted by NRH model and observation values of photosynthetic parameters for seven species under various conditions (mean ± *SE*, *n* = 3-6).

	A. alba				*O. sativa*				*T. aestivum*			
	LL		HL		Wufengyou 1326		Ganfengyou 1326		2% O_2		21% O_2	
	NRH model	Obs.	NRH model	Obs.	NRH model	Obs.	NRH model	Obs.	NRH model	Obs.	NRH model	Obs.
α	0.467 ±0.013	–	0.389 ± 0.045	–	0.248 ± 0.033	-	0.238 ± 0.053	–	0.222 ± 0.028	–	0.269 ± 0.010	–
θ	0.851 ±0.018	–	0.925 ±0.016	–	0.957 ±0.015	–	0.965 ±0.017	–	0.968 ± 0.007	–	0.965 ± 0.010	–
I_{sat}	–	796.00 ±157.46	–	1094.20 ±141.40	–	1133.82 ±133.12	–	1200.59 ±199.73	–	1400.00 ± 141.42	–	1840.00 ± 74.83
J_{max}	95.99 ±9.54^a	94.99 ±5.31^a	127.32 ±4.99^a	127.87 ±3.76^a	111.40 ±2.59^a	113.64 ±2.17^a	93.45 ±1.79^a	105.50 ±7.39^a	159.59 ± 8.82^a	158.08 ± 7.69^a	277.75 ± 8.30^a	248.12 ± 8.39^b
R^2	0.994	–	0.996	–	0.987	–	0.937	–	0.997	–	0.999	–
	S. italica				*Z. mays*		*A. hypochondriacus*		*M. aeruginosa*			
	Normal water		Drought stress						NO^-_3-N		NH_4^+-N	
	NRH model	Obs.	NRH model	Obs.	NRH model	Obs.	NRH model	Obs.	NRH model	Obs.	NRH model	Obs.
α	0.262 ± 0.009	–	0.148 ± 0.008	–	0.275 ± 0.001	–	0.263 ± 0.003	–	0.041 ± 0.000	-	0.038 ± 0.000	–
θ	0.960 ± 0.023	–	0.872 ± 0.064	–	0.901 ±0.010	–	0.893 ±0.006	–	0.955 ± 0.001	–	0.969 ± 0.002	–
I_{sat}	–	1399.75 ± 198.60	–	601.07 ± 0.31	–	1666.67 ±176.38	–	1933.33 ±67.02	–	949.00 ±116.00	–	833.00 ±0.00
J_{max}	155.73 ± 20.11^a	158.72 ± 15.29^a	48.43 ± 11.12^a	48.19 ± 8.89^a	118.33 ±1.53^a	113.95 ±1.02^a	412.63 ±11.23^a	342.91 ±8.02^b	14.12 ±0.14^b	15.65 ±0.61^a	11.86 ±0.50^a	12.99 ±0.49^a
R^2	0.990	–	0.998	–	0.999	–	0.999	–	0.931	–	0.926	–

θ, the convexity (dimensionless); for other abbreviations, see Table 2. The different superscript letters followed by the values are significantly different between fitted values and observation values for the same species or for the same species under the same treatment ($p < 0.05$).

In addition, this model fails to accurately represent the distinct characteristics of the *J–I* curves observed in *A. alba* (Figure 3A), *O. sativa* (Figure 3B), and *M. aeruginosa* (Figure 3F), where the *J–I* curves evidently exhibit a decline as *I* increases beyond I_{sat}. However, compared with the DE and NRH models, our results show that the mechanistic model not only simulates well ($R^2 \geq 0.994$) all the *J–I* curves for different photosynthesis organisms under various environmental conditions (Figures 1-3), but also provides both J_{max} and I_{sat} which are very close to the corresponding observed values (Table 2; Supplementary Table S2).

Discussion

According to Ralph and Gademann (2005), the Chl *a* fluorescence transient *J–I* curves of algae and cyanobacteria may be divided into three distinct parts depending on the level of light intensity used to illuminate the samples; these include light-limited, light-saturated, and photoinhibitory regions/dynamic down-regulation of PSII. We refer the readers to the *J–I* curves of plants, i.e., the section without light-saturated region in *T. aestivum* grown at 21% O_2 (Figures 1C, 2C, 3C), in *A. hypochondriacus* grown under normal conditions (Figures 1E, 2E, 3E), but without obvious photoinhibitory regions/dynamic down-regulation of PSII for *S. italica* grown under drought stress (Figures 1D, 2D, 3D), and in *Z. mays* grown under normal conditions (Figures 1E, 2E, 3E). These results indicate that the *J–I* curves of plants are much more complex compared to those of algae and cyanobacteria. The main reason for this difference is considered to be related to the living environment and evolution of plants and algae. Algae have evolved to adapt to low-intensity light in aquatic environments over a long period of time, and therefore, their saturation light intensity is generally lower than 1000 μmol photons m^{-2} s^{-1} (Ralph and Gademann, 2005; Karageorgou and Manetas, 2006; Yang et al., 2023). On the other hand, plants have evolved differently to adapt to terrestrial environments, leading to significant differences in their saturation light intensity. In this study, the saturation light intensity for *S. italica* grown under drought stress fitted by the mechanistic model was 737.78 μmol photons m^{-2} s^{-1}, while for *A. hypochondriacus* grown under normal conditions it was as high as 2100.22 μmol photons m^{-2} s^{-1} (Table 2). Therefore, when measuring *J-I* curves, if the

experimental conditions set the light intensity below 2000 μmol photons m^{-2} s^{-1}, The *J-I* curves of some plant species may not show obvious photoinhibitory regions/dynamic down-regulation of PSII. Similar findings have also been observed previously on *Capsicum annuum* L. and *Laminaria hyperborea* [(Gunnerus) Foslie, 1884] (Liang et al., 2018; Yang et al., 2018).

Although many models of the *J–I* curves have been developed over the years (Stirbet et al., 2024), it is still unclear what criteria a model should fulfill to be considered as close to a perfect one. To our knowledge, a complete model for the *J–I* curves should meet all the following requirements. It should (1) give good fits for all types of *J–I* curves for photosynthetic organisms under different environmental conditions; (2) provide estimates of photosynthetic parameters (e.g., I_{sat} and J_{max}) that are close to the corresponding measured values without any significant differences; and (3) provide the parameters or coefficients that have clear biological significance. Although the EP model has been considered to be an excellent model for fitting *J-I* curves of algae and phytoplankton, and incorporated into chlorophyll fluorescence instruments (WalZ, Germany), providing parameters such as the maximum rate of photosynthetic production (P_m), the optimal and characteristic light intensities (I_m and I_k), and α, but it has rarely been used for fitting the *J-I* curves of plants (Eilers and Peeters, 1988; Schreiber and Klughammer, 2013). However, this model fails to accurately represent the distinct characteristic of the *J-I* curves observed in *O. sativa* cv Ganfengyou 1326 grown under normal condition and *M. aeruginosa* grown under different nitrogen treatments, where the *J-I* curves evidently exhibit a decline as *I* increases beyond I_{sat} (Supplementary Figure S1). Furthermore, unlike the DE and EP models which are constructed with photosynthetic factory or photosynthetic units as the basic unit (Platt et al., 1980; Eilers and Peeters, 1988), the mechanistic model is built based on individual photosynthetic pigment molecules (Ye et al., 2013a, b). In addition to accurately and precisely calculate the parameters of J_{max} and I_{sat} for different photosynthetic organisms under various environmental conditions (Table 2), the mechanistic model can also obtain certain parameters that reflect the intrinsic characteristics of photosynthetic pigment molecules, such as the number of photosynthetic pigment molecules in the excited state (N_k), the eigen-absorption cross-section of photosynthetic pigment molecule from ground state *i* to excited state *k* (σ_{ik}), the effective optical absorption cross-section of photosynthetic pigment molecule from ground state *i* to excited state *k* (σ'_{ik}), and the minimum average life-time of photosynthetic pigment molecules in the excited state *k* (τ_{min}) (Ye et al., 2013b, 2019; He et al., 2020). The mechanistic models can not only fit the *J/I* curves of algae (Liang et al., 2018; Yang et al., 2023), but also fit the *J/I* curves of higher plants under various environmental conditions (Sun et al., 2015; He et al., 2020; Ye et al., 2020; Wang et al., 2022). Therefore, based on the fact that the DE, EP, and NRH models are only applicable to either algae or plants and provide limited parameters, the mechanistic model has the potential to become an ideal model for fitting *J-I* curves of different photosynthetic organisms (including C_3, C_4 plants and algae) under various environmental conditions.

A number of studies have previously compared the parameters obtained from different *J–I* models in algae and cyanobacteria (Jassby and Platt, 1976; Frennette et al., 1993). Alternative models, such as the DE model, have given different fitting effects (Frennette et al., 1993; Yang et al., 2018). Previous studies have indicated that the fitting performance of the DE model in estimating J_{max} and I_{sat} mainly depends on whether dynamic down-regulation of the PSII occurs in plants, algae and cyanobacteria (Suggett et al., 2007; Buckley and Diaz-Espejo, 2015). In this study, our results show that the DE model can fit the *J–I* curves well for all the studied species, regardless of photoinhibition/dynamic down-regulation of PSII (Figure 1); however, this model significantly overestimates both I_{sat} and J_{max} for *A. hypochondriacus* grown under normal conditions and underestimates I_{sat} for *M. aeruginosa* grown under NH^+_4-N supply (Table 3, Supplementary Table S2). More importantly, although J_s is termed as the maximum, potential, light saturated *J*, the values of J_s estimated by this model are significantly greater than the observed values of J_{max} except for *S. italica* gown under drought stress and *O. sativa* cv Ganfengyou 1326 grown under normal conditions, specially, for *T. aestivum* (grown at 2% O_2 and 21% O_2), *Z. mays* (grown under normal conditions), and *M. aeruginosa* (grown under different nitrogen treatments) (Table 3). For instance, when *T. aestivum* is grown at 21% O_2, the value of J_s estimated by the DE model is 1.10×10^7 μmol photons m^{-2} s^{-1}, whereas the observed value of J_{max} is 248.12 (± 8.39) μmol photons m^{-2} s^{-1}. In addition, if *J–I* curves of *T. aestivum* at 21% O_2 are fitted by the single exponential model, the value of J_{max} is 280.25 μmol photons m^{-2} s^{-1}. Previous studies suggest that although the J_s in plants and algae vary among different species and environmental conditions, its value is generally expected to be the similar to J_{max} and lower than 10^3 μmol electrons m^{-2} s^{-1} (Buckley and Farquhar, 2004; Baker, 2008; Feng et al., 2022). In our study, however, the value of J_s is unexpectedly high attaining up to 10^8 μmol electrons m^{-2} s^{-1} (Table 3). On the other hand, for *O. sativa* cv Ganfengyou 1326 (grown under normal conditions), J_s estimated by the DE model is 75.56 (±5.89) μmol photons m^{-2} s^{-1}, which is significantly lower than its observed value of J_{max} (105.50 (±7.39) μmol photons m^{-2} s^{-1}) (Table 3). Some other studies have also indicated that J_s in the DE model is not a potentially real J_{max}, but only a coefficient without any biological significance, and the role of the parameter introduced for J_s in Equation 6 is simply to facilitate the calculation of J_{max} and I_{sat} (Buckley and Farquhar, 2004; Suggett et al., 2007). To our knowledge, there are only a few case studies in which the values of J_s have been reported when the *J–I* curves of algae and cyanobacteria were simulated by the DE model (Suggett et al., 2007; Buckley and Diaz-Espejo, 2015; Liang et al., 2018). The possible reason why J_s has rarely been discussed in the literature may be due to the challenges in explaining its biological meaning when its value is evidently higher or lower than the observed J_{max}.

The value of photoinhibition coefficient (β) in the DE model may vary in different photosynthetic organisms under various environmental conditions (Harrison and Platt, 1986). Generally, the value of β falls within the range of 0.05 to 0.2 μmol electrons $(\mu mol\ photons)^{-1}$ (Harrison and Platt, 1986; Ralph and Gademann, 2005). However, our results demonstrate that the estimated value of β obtained from fitting the DE model is exceptionally high, reaching

up to 10^5 for *M. aeruginosa* grown under NO^-_3-N supply, as presented in Table 3. Similar to the J_s, it is challenging to comprehend the biological significance of β in the DE model. Consequently, the DE model is not an appropriate model for fitting *J–I* curves and for estimating J_{max} and I_{sat}, as well as for interpreting the biological significance of coefficients J_s and β in the model.

The NRH model has been a sub-model in the FvCB model when irradiance is below the saturation level (Long and Bernacchi, 2003; Buckley and Farquhar, 2004; Sharkey et al., 2007; Miao et al., 2009; Yin et al., 2009; Gu et al., 2010; Bernacchi et al., 2013; von Caemmerer, 2013; Park et al., 2016; Cai et al., 2018; Yin et al., 2021). This model has been widely used in studies on various C_3 plants under different environmental conditions, but it has been rarely used to fit the *J–I* curves of algae and cyanobacteria (von Caemmerer, 2000; Long and Bernacchi, 2003; Miao et al., 2009; Gu et al., 2010; Bernacchi et al., 2013; von Caemmerer, 2013; Buckley and Diaz-Espejo, 2015; Cai et al., 2018; Yin et al., 2021). In this study, we find that this model can well simulate the *J–I* curves without PSII dynamic down-regulation/photoinhibition in *T. aestivum* at two different O_2 concentrations (Figure 3C), in *S. italica* grown under drought stress (Figure 3D), and in *Z. mays* and *A. hypochondriacus* grown under normal conditions (Figure 3E), all with extremely good fits (R^2≥0.997), but it poorly characterizes the *J–I* curves with PSII dynamic down-regulation/photoinhibition for *A. alba* under HL (Figure 3A), *O. sativa* grown under normal conditions (Figure 3B) and *M. aeruginosa* under different nitrogen treatments (Figure 3F). The reason behind this mainly lies in the fact that the NRH model is a function without a maximum value, representing an asymptotic line without inflection points. As a result, the NRH model can poorly characterize the *J–I* curves of higher plant species and of algae with PSII dynamic down-regulation/photoinhibition. In addition, for *T. aestivum* grown at 21% O_2 concentration (Figure 3C), and for *A. hypochondriacus* grown under normal conditions (Figure 3E) without PSII dynamic down-regulation/photoinhibition, the NRH model overestimates the values of J_{max}, especially for *A. hypochondriacus* grown under normal conditions (Tables 4, S2). The fitted results, depicted here, are consistent with the findings of earlier studies (Buckley and Diaz-Espejo, 2015; Ye et al., 2019). Meanwhile, this model underestimates the J_{max} for *M. aeruginosa* grown under NO^-_3-N supply (Table 4; Supplementary Table S2). In addition, for *A. alba* grown under HL and LL (Figure 3A), *O. sativa* grown under normal conditions (Figure 3B), *S. italica* grown under drought stress (Figure 3D) and *M. aeruginosa* grown under NO_3^-N and NH_4^+-N supplies (Figure 3F), the curves fitted by the NRH model deviate from the measurements on the *J–I* curves, especially for *M. aeruginosa* (Figure 3F). More importantly, this model fails to estimate I_{sat} accurately due to its asymptote nature without an extreme value. At the same time, the NRH model is also unsuitable for accurately estimating the values of J_{max} and determining the value of I_{sat} (Table 4, Supplementary Table S2). Therefore, we can conclude that the NRH model is not a good choice for fitting the *J–I* curves.

Although the EP model is primarily used to fit *I* response to the rate of photosynthesis (Eilers and Peeters, 1988; Schreiber and Klughammer, 2013), it can also be used to fit *J-I* curves for different photosynthetic organisms if photosynthesis is replaced by electron transport rate (*J*). From the fitting results of this study, it can be seen that the EP model can fit the *J-I* curves of plants or algae under photoinhibition/dynamic down-regulation (Supplementary Figure S1). For example, the EP model can fit the *J-I* curves of Ganfengyou 1326 (R^2 = 0.973) and *M. aeruginosa* (R^2 = 0.976 or 0.989) under photoinhibition/dynamic down-regulation, and the fitting coefficients for the *J-I* curves of other plants in this study showed extremely good fits (R^2 ≥ 0.996). Furthermore, except for significantly overestimating the values of I_{sat} for *A. hypochondriacus* grown under normal conditions, and significantly underestimating the values of I_{sat} for *M. aeruginosa* grown under NH_4^+-N supply (Supplementary Tables S1, S2), the values of J_{max} and I_{sat} fitted by the EP model were very close to their corresponding observed values for the other plant species (Supplementary Table S1). However, considering that the EP model, like the DE, is based on the photosynthetic factory or photosynthetic unit as the basic unit, the relationship between these coefficients of *k*, α, β, γ, and δ in the model and the characteristics of photosynthetic pigment molecules are unknown (Eilers and Peeters, 1988). In addition, we found that *b* is a negative value for *A. hypochondriacus*, and it must be positive in the model (Eilers and Peeters, 1988). Consequently, it is not a perfect model for fitting *J-I* curves of different photosynthetic organisms under various environmental conditions.

Compared with the DE and NRH models, fitting the mechanistic model to previously collected data not only yielded excellent fits (R^2≥0.994), but also provided the values of J_{max} and I_{sat} which were very close to their corresponding observed values (Table 2). Moreover, no significant differences were found between the fitted values for J_{max} (and I_{sat}) and their corresponding observed values (p< 0.05; Table 2). Our results are consistent with the findings of earlier studies (Ye et al., 2013a, 2016; Robakowski et al., 2018; Yang et al., 2018; Ye et al., 2019; Zuo et al., 2019; Ye et al., 2020; Hu et al., 2021; He et al., 2022; Robakowski et al., 2022; Yang et al., 2023). In addition, previous results have also demonstrated that this model is suitable for fitting the *J–I* curves of algae and cyanobacteria (Ye et al., 2013a; Liang et al., 2018; Yang et al., 2023). The aforementioned results indicate that the mechanistic model is not only appropriate for fitting the *J–I* curves, but also for estimating the values of both J_{max} and I_{sat} regardless of the dynamic down-regulation/photoinhibition in different photosynthetic organism under various environmental conditions. In addition, the three coefficients (i.e., α, β and γ) in the model have clear biological significance. Our results, in this study, demonstrate that the mechanistic model is much more universal than both the NRH and DE models; therefore, it is the optimal option for fitting *J–I* curves (Figures 1-3), and for estimating the values of J_{max} and of I_{sat} for different photosynthetic organisms under various environmental conditions (Tables 2-4).

In conclusion, our results show that the mechanistic model can address the limitations observed in both the DE and NRH models. Our current study highlights the robustness of the mechanistic model in accurately characterizing the *J–I* curves of seven species under various environmental conditions (Figures 1-3).This contributes significantly to our comprehension of leaf-scale

modelling of *J–I* relations, especially in (**1**) reproducing the entire curves from low to high *I* levels for different photosynthetic organisms under various environmental conditions, and (**2**) obtaining key measurable parameters (e.g., J_{max} and I_{sat}) derived from the *J–I* curve for different plants, algae and cyanobacteria, grown under various environmental conditions (Table 2).

To facilitate the utilization of our mechanistic model of the *J–I* curve by other researchers, we have developed and exploited a *Photosynthesis Model Simulation Software* (PMSS) with both Chinese and English versions (http://photosynthetic.sinaapp.com). In PMSS, users can access various models (including classical model, such as rectangular hyperbolic model, non-rectangular hyperbolic model, exponential model, double exponential model, Eilers-Peeters model), e.g., light and CO_2-response models of photosynthesis, electron transport rate, instantaneous water-use efficiency (defined as A/T_r; A, net photosynthesis rate; T_r, transpiration rate), and intrinsic water-use efficiency (defined as A/g_s; A, net photosynthesis rate; g_s, stomatal conductance). These models are useful mathematical tools for studying the photosynthetic characteristics of plants, algae, and cyanobacteria, as well as for estimating their key photosynthetic parameters.

Data availability statement

The original contributions presented in the study are included in the article/Supplementary Material. Further inquiries can be directed to the corresponding authors.

Author contributions

Z-PY: Conceptualization, Formal Analysis, Funding acquisition, Resources, Writing – original draft, Writing – review & editing. TA: Data curation, Investigation, Writing – review & editing. GG: Writing – review & editing. PR: Data curation, Investigation, Writing – review & editing. AS: Data curation, Investigation, Writing – review & editing. X-LY: Investigation, Visualization, Writing – review & editing. X-YH: Data curation, Investigation, Writing – review & editing. H-JK: Conceptualization, Data curation, Formal Analysis, Investigation, Writing – review & editing. F-BW: Conceptualization, Data curation, Investigation, Writing – original draft, Writing – review & editing.

Funding

The author(s) declare financial support was received for the research, authorship, and/or publication of this article. This research was supported by the Natural Science Foundation of China (Grant No. 32260063 and 31960054), and the Natural Science Foundation of Jiangxi Province (Grant No.20224BAB205020).

Acknowledgments

Govindjee acknowledges computational help he received from the office of Information Technology of the School of Integrative Biology, University of Illinois at Urbana- Champaign.

Conflict of interest

The authors declare that the research was conducted in the absence of any commercial or financial relationships that could be construed as a potential conflict of interest.

Publisher's note

Supplementary material

The Supplementary Material for this article can be found online at: https://www.frontiersin.org/articles/10.3389/fpls.2024.1332875/full#supplementary-material

References

Ahammed, G. J., Xu, W., Liu, A., and Chen, S. (2018). COMT1 silencing aggravates heat stress-induced reduction in photosynthesis by decreasing chlorophyll content, photosystem II activity and electron transport efficiency in tomato. *Front. Plant Sci.* 9. doi: 10.3389/fpls.2018.00998

Baker, N. R. (2008). Chlorophyll fluorescence: a probe of photosynthesis in *vivo*. *Annu. Rev. Plant Biol.* 59, 89–113. doi: 10.1146/annurev.arplant.59.032607.092759

Bernacchi, C. J., Bagley, J. E., Serbin, S. P., Ruiz-Vera, U. M., Rosenthal, D. M., and Vanloocke, A. (2013). Modelling C_3 photosynthesis from the chloroplast to the ecosystem. *Plant Cell Environ.* 36, 1641–1657. doi: 10.1111/pce.12118

Buckley, T. N., and Diaz-Espejo, A. (2015). Reporting estimates of maximum potential electron transport rate. *New Phytol.* 205, 14–17. doi: 10.1111/nph.13018

Buckley, T. N., and Farquhar, G. D. (2004). A new analytical model for whole-leaf potential electron transport rate. *Plant Cell Environ.* 27, 1487–1502. doi: 10.1111/j.1365-3040.2004.01232.x

Cai, C., Li, G., Yang, H. L., Yang, J., Liu, H., Struik, P. C., et al. (2018). Do all leaf photosynthesis parameters of rice acclimate to elevated CO_2, elevated temperature, and their combination, in FACE environments? *Global Change Biol.* 24, 1685–1707. doi: 10.1111/gcb.13961

Chang, T. G., Wei, Z. W., Shi, Z., Xiao, Y., Zhao, H., Chang, S. Q., et al. (2023). Bridging photosynthesis and crop yield formation with a mechanistic model of whole-plant carbon nitrogen interaction. *Plants* 5, 1–19. doi: 10.1093/insilicoplants/diad011

Eilers, P. H. C., and Peeters, J. C. H. (1988). A model for the relationship between light internsity and the rate of photosynthesis in phytoplankton. *Ecol. Model.* 42, 199–215. doi: 10.1016/0304-3800(88)90057-9

Farquhar, G. D., von Caemmerer, S., and Berry, J. A. (1980). A biochemical model of photosynthetic CO_2 assimilation in leaves of C_3 species. *Planta* 149, 78–90. doi: 10.1007/bf00386231

Feng, Y. N., Wang, Y. B., Ren, H. F., Zhang, D. S., Zong, Y. Z., Shi, X. R., et al. (2022). Mechanism of the effect of elevated CO_2 concentration on mitigating drought stress in foxtail millet. *J. China Agr Univ* 27, 43–57. doi: 10.11841/j.issn.1007-4333

Frenette, J. J., Demers, S., Legendre, L., and Dodson, J. (1993). Lack of agreement among models for estimating the photosynthetic parameters. *Limnol Oceanogr.* 38, 679–687. doi: 10.4319/lo.1993.38.3.0679

Govindjee, G. (1990). Photosystem II heterogeneity: the acceptor side. *Photosynth Res.* 25, 151–160. doi: 10.1007/bf00033157

Govindjee, G. (2004). "Chlorophyll a fluorescence: a bit of basics and history," in *chlorophyll a fluorescence: a signature of photosynthesis*. Eds. G. C. Papageorgiou and Govindjee, (Kluwer Academic (now Springer, Dordrecht, Netherlands), 1–42.

Gu, L., Pallardy, S. G., Tu, K., Law, B. E., and Wullschleger, S. D. (2010). Reliable estimation of biochemical parameters from C_3 leaf photosynthesis-intercellular carbon dioxide response curves. *Plant Cell Environ.* 33, 1852–1874. doi: 10.1111/j.1365-3040.2010.02192.x

Harrison, W. G., and Platt, T. (1986). Photosynthesis-irradiance relationships in polar and temperate phytoplankton populations. *Polar Biol.* 5, 153–164. doi: 10.1007/BF00441695

He, L., Luo, H., He, X. P., Bian, J. M., Zhu, C. L., Fu, J. R., et al. (2020). Photosynthetic characteristics of different super early rice based on mechanistic model of light-response of photosynthetic electron flow. *J. Nucl Agr Sci* 34, 418–424. doi: 10.11869/j.issn.100-8551.2020.02.0418

He, Y. L., Wu, Y., Ye, Z. P., Zhou, S. X., Ye, S. C., and Liu, W. X. (2022). Response of intrinsic characteristics of light-harvesting pigment molecules, light use efficiency to light intensity for oil-tea (*Camellia oleifera*). *Acta Bot. Boreali-Occidential Sin.* 42, 1552–1560. doi: 10.7606/j.issn.1000-4025.2022.09.1552

Henley, W. J. (1993). Measurement and interpretation of photosynthesis light-response curves in algae in the context of photoinhibition and diel changes. *J. Phycol* 29, 729–739. doi: 10.1111/j.0022-3646.1993.00729.x

Hu, W. H., Xiao, Y. A., Yan, X. H., Ye, Z. P., Zeng, J. J., and Li, X. H. (2021). Photoprotective mechanisms under low temperature and high light stress of *Photinia* × *fraseri* and *Osmanthus fragrans* during overwintering. *Bull. Bot. Res.* 41, 938–946. doi: 10.7525/j.issn.1673-5102.2021.06.012

Jassby, A. D., and Platt, T. (1976). Mathematical formulation of the relationship between photosynthesis and light for phytoplankton. *Limnol Oceanogr* 21, 540–547. doi: 10.4319/lo.1976.21.4.0540

Kang, H. J., Duan, S. H., An, T., and Ye, Z. P. (2019). Estimation of maximum electron transport rate of wheat based on FvCB model. *J. Triticeae Crops* 39, 1377–1384. doi: 10.7606/j.issn.1009-1041.2019.11.14

Karageorgou, P., and Manetas, Y. (2006). The importance of being red when young: anthocyanins and the protection of young leaves of *Quercus coccifera* from insect herbivory and excess light. *Tree Physiol.* 26, 613–621. doi: 10.1093/treephys/26.5.613

Liang, Z. R., Liu, F., Yuan, Y. M., Du, X. X., Wang, W. J., and Sun, X. T. (2018). Effect of different temperatures on growth and photosynthetic characteristic of *Laminaria hyperborea* young seedling. *Mar. Sci.* 42, 71–78. doi: 10.11759/hykx20171121003

Long, S. P., and Bernacchi, C. J. (2003). Gas exchange measurements, what can they tell us about the underlying limitations to photosynthesis? Procedures and sources of error. *J. Exp. Bot.* 54, 2393–2401. doi: 10.1093/jxb/erg262

Mar, T., and Govindjee, G. (1972). Kinetic models of oxygen evolution in photosynthesis. *J. Theor. Biol.* 36, 427–446. doi: 10.1016/0022-5193(72)90001-x

Maxwell, K., and Johnson, N. G. (2000). Chlorophyll fluorescence-a practical guide. *J. Exp. Bot.* 51, 659–668. doi: 10.1093/jexbot/51.345.659

Miao, Z., Xu, M., Lathrop, R. G., and Wang, Y. (2009). Comparison of the A–C_c curve fitting methods in determining maximum ribulose-1, 5-bisphosphate carboxylase/oxygenase carboxylation rate, potential light saturated electron transport rate and leaf dark respiration. *Plant Cell Environ.* 32, 109–122. doi: 10.1111/j.1365-3040.2008.01900.x

Morfopoulos, C., Sperlich, D., Peñuelas, J., Filella, I., Llusià, J., and Medlyn, B. E. (2014). A model of plant isoprene emission based on available reducing power captures responses to atmospheric CO_2. *New Phytol.* 203, 125–139. doi: 10.1111/nph.12770

Park, K. S., Kim, S. K., Cho, Y. Y., Cha, M. K., Jung, D. H., and Son, J. E. (2016). A coupled model of photosynthesis and stomatal conductance for the ice plant (*Mesembryanthemum crystallinum* L.), a facultative CAM plant. *Hortic. Environ. Biote* 57, 259–265. doi: 10.1007/s13580-016-0027-7

Platt, T., Gallegos, C. L., and Harrison, W. G. (1980). Photoinhibition of photosynthesis in natural assemblages of marine phytoplankton. *J. Mar. Res.* 38, 687–701. doi: 10.1093/pasj/57.2.341

Ralph, P. J., and Gademann, R. (2005). Rapid light curves: a powerful tool assess photosynthetic activity. *Aquat Bot.* 82, 222–237. doi: 10.1016/j.aquabot.2005.02.006

Rascher, U., Liebieg, M., and Lüttge, U. (2000). Evaluation of instant light-response curves of chlorophyll fluorescence parameters obtained with a portable chlorophyll fluorometer on site in the field. *Plant Cell Environ.* 23, 1397–1405. doi: 10.1046/j.1365-3040.2000.00650.x

Robakowski, P. (2005). Susceptibility to low-temperature photoinhibition in three conifers differing in successional status. *Tree Physiol.* 25, 1151–1160. doi: 10.1093/treephys/25.9.1151

Robakowski, P., Łukowski, A., Ye, Z. P., Kryszewski, A., and Kowalkowski, W. (2022). Northern provenances of silver fir differ with acclimation to contrasting light regimes. *Forests* 13, 1164. doi: 10.3390/f13081164

Robakowski, P., Pers-Kamczyc, E., Ratajczak, E., Thomas, P. A., Ye, Z. P., Rabska, M., et al. (2018). Photochemistry and antioxidative capacity of female and male *Taxus baccata* L. acclimated to different nutritional environments. *Front. Plant Sci.* 9. doi: 10.3389/fpls.2018.00742

Schreiber, U., and Klughammer, C. (2013). Wavelength-dependent photodamage to Chlorella investigated with a new type of multi-color PAM chlorophyll fluorometer. *Photosynth Res.* 114, 165–177. doi: 10.1007/s11120-013-9801-x

Serodio, J., Ezequiel, J., Frommlet, J., Laviale, M., and Lavaud, J. (2013). A method for the rapid generation of nonsequential light-response curves of chlorophyll fluorescence. *Plant Physiol.* 163, 1089–1102. doi: 10.1104/pp.113.225243

Sharkey, T. D., Bernacchi, C. J., Farquhar, G. D., and Singsaas, E. L. (2007). Fitting photosynthetic carbon dioxide response curves for C_3 leaves. *Plant Cell Environ.* 30, 1035–1040. doi: 10.1111/j.1365-3040.2007.01710.x

Shevela, S., Kern, J. F., Govindjee, G., and Messinger, J. (2023). Solar energy conversion by photosystem II: principles and structures. *Photosynth Res.* 156, 279–307. doi: 10.1007/s11120-022-00991-y

Stirbet, A., Guo, Y., Lazár, D., and Govindjee, G. (2024). From leaf to multiscale models of photosynthesis: Applications and challenges for crop improvement. *Photosynth. Res.*, in the press, # dOc4fc9c_eO8e_4efa

Stirbet, A., Lazár, D., Guo, Y., and Govindjee, G. (2020). Photosynthesis: basics, history and modelling. *Ann. Bot.* 126, 511–537. doi: 10.1093/aob/mcz171

Suggett, D. J., Le Floc'H, E., Harris, G. N., Leonardos, N., and Geider, R. J. (2007). Different strategies of photoacclimation by two strains of *Emiliania huxleyi* (haptophyta). *J. Phycol* 43, 1209–1222. doi: 10.1111/j.1529-8817.2007.00406.x

Sun, J., Sun, J., and Feng, Z. (2015). Modelling photosynthesis in flag leaves of winter wheat (*Triticum aestivum*) considering the variation in photosynthesis parameters during development. *Funct. Plant Biol.* 42, 1036–1044. doi: 10.1071/FP15140

von Caemmerer, S. (2000). *Biochemical models of leaf photosynthesis. Vol. 2* (Collingwood, Australia: CSIRO Publishing).

von Caemmerer, S. (2013). Steady-state models of photosynthesis. *Plant Cell Environ.* 36, 1617–1630. doi: 10.1111/pce.12098

Wang, X., Yang, X. L., Ye, Z. P., Lu, Y. T., and Ma, X. F. (2022). Stomatal and non-stomatal limitations to photosynthesis in *Sorghum bicolor* at different temperatures. *Plant Physiol. J.* 58, 1245–1253. doi: 10.13592/j.cnki.ppj.2021.0403

White, A. J., and Critchley, C. (1999). Rapid light curves: a new fluorescence method to assess the state of the photosynthetic apparatus. *Photosynth Res.* 59, 63–72. doi: 10.1023/A:1006188004189

Yang, X. L., Dong, W., Liu, L. H., Bi, Y. H., Xu, W. Y., and Wang, X. (2023). Uncovering the differential growth of *Microcystis aeruginosa* cultivated under nitrate and ammonium from a photophysiological perspective. *ACS EST Water* 3, 1161–1171. doi: 10.1021/acsestwater.2c00624

Yang, X. M., Wu, X. L., Liu, Y. F., Li, T. L., and Qi, M. (2018). Analysis of chlorophyll and photosynthesis of a tomato chlorophyll-deficient mutant induced by EMS. *Chin. J. Appl. Ecol.* 29, 1983–1989. doi: 10.13287/j.1001-9332.201806.021

Ye, Z. P., Hu, W. H., Yan, X. H., and Duan, S. H. (2016). Photosynthetic characteristics of different plant species based on a mechanistic model of light-response of photosynthesis. *Chin. J. Ecol.* 35, 2544–2552. doi: 10.13292/j.1000-4890.201609.032

Ye, Z. P., Ling., Y., Yu, Q., Duan, H. L., and Zhou, S. X. (2020). Quantifying light response of leaf-scale water-use efficiency and its interrelationships with photosynthesis and stomatal conductance in C_3 and C_4 Species. *Front. Plant Sci.* 11. doi: 10.3389/fpls.2020.00374

Ye, Z. P., Robakowski, P., and Suggett, D. J. (2013a). A mechanistic model for the light response of photosynthetic electron transport rate based on light harvesting properties of photosynthetic pigment molecules. *Planta* 237, 837–847. doi: 10.1007/s00425-012-1790-z

Ye, Z. P., Suggett, D. J., Robakowski, P., and Kang, H. J. (2013b). A mechanistic model for the photosynthesis–light response based on the photosynthetic electron transport of photosystem II in C_3 and C_4 species. *New Phytol.* 199, 110–120. doi: 10.1111/nph.12242

Ye, Z. P., Yin, J. H., Chen, X. M., An, T., and Duan, S. H. (2019). Investigation on photosynthetic characteristics of flag leaves of several hybrid rice cultivars in dough stage. *Acta Agr Zhejiangensis* 31, 355–364. doi: 10.3969/j.issn.1004-1524.2019.03.02

Yin, X., Busch, F. A., Struik, P. C., and Sharkey, T. D. (2021). Evolution of a biochemical model of steady-state photosynthesis. *Plant Cell Environ.* 44, 2811–2837. doi: 10.1111/pce.14070

Yin, X. Y., Struik, P. C., Romero, P., Harbinson, J., Evers, J. B., van der Putten, P. E. L., et al. (2009). Using combined measurements of gas exchange and chlorophyll fluorescence to estimate parameters of a biochemical C_3 photosynthesis model: a critical appraisal and a new integrated approach applied to leaves in a wheat (*Triticum aestivum*) canopy. *Plant Cell Environ.* 32, 448–464. doi: 10.1111/j.1365-3040.2009.01934.x

Zuo, G. Q., Wang, S. Y., Feng, N. J., Wang, X. X., Mu, B. M., and Zheng, D. F. (2019). Effects of uniconazole on photosynthetic physiology and phenotype of soybean under flooding stress. *Chin. J. Ecol.* 38, 2702–2708. doi: 10.13292/j.1000-4890.201909.029